Fully-Adaptive Update Rate for Nonlinear Trackers

M Pilté, Silvere Bonnabel, F Barbaresco

Fully-Adaptive Update Rate for Nonlinear Trackers

M. Pilté[1,2], S. Bonnabel[1], and F. Barbaresco[2]

[1]Mines ParisTech, PSL University, 60 boulevard Saint-Michel, 75006 Paris
[2]Thales Air Systems, Voie Pierre Gilles de Gennes, Hameau de Roussigny, 91470 Limours

Abstract

Modern phased-array multifunction radars have the ability to change or schedule the tasks of the beam in order to accomplish all their missions in an optimized fashion. The resource manager of the radar must then control the update rate of the measurement task of target active tracking, so as to minimize the radar computer load without losing targets. Scarce measurements lead to low radar load, but they also lead to an increased number of illuminations at each measurement epoch to find the target. Based upon this rationale, a sound procedure was proposed by Blackman and Van Keuk to derive an optimal measurement rate. Their optimization criterion is established using a linear Singer target model and a linear Kalman filter. In this paper their method is extended, and we propose a versatile optimal update rate algorithm that is applicable to virtually any nonlinear target model combined with any nonlinear filter able to output an error covariance matrix. This includes EKF, UKF, IMM, and particle filters. For numerical experiments and validation we consider a nonlinear target model based on Frenet-Serret 3D equations, and the tracking is performed by a nonlinear Invariant Extended Kalman Filter (IEKF).

1 Introduction

The idea of cognitive radar has been defined in [2], and further developed in [3]. The ability to adjust the illuminations in an intelligent manner is one of the characteristics that distinguishes a cognitive radar from an adaptive one. Update rate adaptation falls into this category. Indeed, the beam can be controlled to illuminate the most interesting regions of the space in an intelligent manner, so that radar time budget is saved and tracks are all maintained. This is possible thanks to the emergence of phased-array fixed antennas that allow illuminating any region of the space at any time, as illuminations are no longer imposed by the rotation of the antenna.

Phased-array multifunction radars are designed to perform several tasks in parallel, such as surveillance, also called Track While Scan (TWS), and active tracking (AT). There is thus a competition between these different tasks regarding the resources of the radar. The role of the resource manager is then to study and organize the different requests. And notably as the radar beam is needed for both TWS and AT, its update frequency for active tracking has to be carefully controlled, as well as for the TWS task. Optimization to cover the entire space during TWS has already been studied, see [4], [5]. In the case of AT, the illuminations requested have a label containing a duration and an update period, and the adaptive resource manager uses a scheduling algorithm to determine in which order these illuminations should be scheduled. Moreover, priority requirements may be accounted for. This priority can for example be the result of a degradation in the tracking performances detected by an update rate adaptation algorithm. Indeed, the radar must definitely not drop a track, especially when performing active tracking. The drop probability, or equivalently the detection probability, are determined in function of the performances of the filtering algorithm used to estimate the target's state, and other fixed characteristics of the radar, such as the Signal to Noise Ratio (SNR) for a beam pointing in the direction of the target.

In this paper, we generalize the sound work of [1] to optimize the update rate of the radar. In [1], the update rate adaptation method is designed for one particular type of target model, namely the Singer model [6], combined with a Kalman tracking algorithm. Since, it has been used as an efficient (yet suboptimal) rule of thumb, even when using a different (possibly nonlinear) target model. Owing to the progresses of computers over the past 25 years, we show it is now possible to extend the method to any target model and estimation algorithm. Moreover, one must bear in mind that the goal of update rate optimization is rather to save radar budget, than to enhance the performances of the state estimation. Nevertheless, the tracking estimation precision has to stay within an acceptable range, as also ensured with the algorithm proposed in this paper.

A Kalman-type filtering algorithm provides the estimated distribution of the state, assuming that this distribution is Gaussian. It thus provides the mean of the distribution, which is usually called the estimated state, and the covariance of the distribution. Among the most well known algorithms are the linear Kalman Filter, the Extended Kalman Filter [10], and the Unscented Kalman Filter [11], [12] for the Kalman-based algorithms. There are also the particle filters, among which [13] for the standard particle filter or [14] for the Rao-Blackwellized particle filter. Although the method of Blackman and Van Keuk relies on a fixed criterion, because of the particular form of the state evolution model chosen, it is possible to compute the detection probability for one target with respect to the covariance output by any of the latter filters in real time. The update rate adaptation introduced in the present paper, that allows for the criterion to adapt over time, builds upon the latter idea.

Target tracking typically relies on an accurate motion model and a robust filtering algorithm. In this paper, the general methodology will be applied to a 3D target model in intrinsic coordinates based on the Frenet-Serret frame. Such kind of nonlinear models are advocated in [7] and appear well suited to actual target motion, since they essentially correspond to piecewise constant command controls in the frame of the target. The filtering algorithm used to estimate the state parameters is called an Invari-

ant Extended Kalman Filter (IEKF). This algorithm is more robust than the standard Extended Kalman Filter (EKF) according to the results of [8] and [**?**] for guidance and navigation applications, and [9] for radar. The proposed update rate adaptation method will be applied to the latter model and filter in the numerical experiment section, but it may in principle be applied to any model combined with any other filtering algorithm that provides a covariance to the user.

1.1 Links with prior literature

To optimize the update rate of observations during Active Tracking, one has to define an optimization problem. In this paper, we use the same criterion as [1], where the authors model the load of the radar as a ratio between the number of illuminations necessary to find a target (at each measurement epoch) and the time elapsed between two measurements. The rationale is that scarce measurements lead to low radar load, but they also lead to an increased number of illuminations at each measurement epoch to find the target. As a result, finding the optimal update rate (i.e., time between two consecutive measurements) is a feasible optimization problem. Other optimization schemes may be designed depending on the radar's performances and on the user's objectives, but in this paper we focus on the optimization problem as posed by Blackman and Van Keuk.

Other update rate adaptation algorithms have been developed in the literature. [15] uses an alpha beta filter and an adaptation scheme so that the residual error of the filter remains constant. Another type of algorithm consists in using an Interacting Multiple Model filtering algorithm (IMM), as in [16], or later [17], where the idea is also to maintain a given level of filtering precision, thanks to the covariances computed by the IMM. The IMM is also used in [18] to control the size of the validation region, to address the association problem. Our problem is slightly different, since we are not only interested in maintaining a given precision, but in reducing the overall radar time spent for each measurement. In [19], the IMM is also used to compute an adaptive update rate related to the maneuvers of the target, and based on the Blackman and Van Keuk approach. However, contrary to the latter, we propose a versatile algorithm that applies to virtually all kinds of filtering algorithms, and we rely on the filter to return necessary mathematical quantities.

Another method to adapt the update rate is to use a maneuver detection algorithm, such as the Variable Rate Particle Filter, see [20], [7], which may be used as a maneuver detector. The Variable Rate Particle Filter is used to evaluate the proportion of jumping particles, and thus is able to detect when more particles are jumping, which means that a parameter is abruptly changing. More generally, change detectors are a very wide class of algorithms, that are described in the book [21], or more precisely in [22] for the Generalized Likelihood Ratio (GLR) algorithm, or [23] for the CUSUM algorithm. Another change detection method based on the computation of appropriate distances between the outputs of Kalman filters can also be designed, as stated in [24]. All these detectors perform quite well when applied with an IMM algorithm. We will not discuss these methods in this paper, since we opted for a wholly different route. Increasing the measurement rate when a change is detected is quite basic, and change detectors are rarely used as update adaptation means but rather as urgent pointing commands.

1.2 Organization and contributions of the paper

This paper is organized as follows. In section 2, we provide a digest of the Blackman-Van Keuk method to optimize the update rate. This section may serve as a tutorial introduction to the more difficult to read paper [1]. The method is generalized in section 3, and results in a versatile adaptive algorithm. More precisely our algorithm informs the radar resource manager what the (maximum) measure update should be in real time so that the detection probability of a given target stays above a given threshold. Then, in section 4, this novel algorithm is applied to a nonlinear target model based on Frenet-Serret equations. The state estimation task is performed by a nonlinear filtering algorithm, the IEKF, which is suits well the considered model. Finally in section 5, the proposed algorithm is compared to the Blackman and Van Keuk criterion, using both the Singer model and the nonlinear model of Section section 4.

2 Fixed update optimization criterion

In this section, we first recall the equations of the Singer target model and of the linear Kalman filter. This model is needed to derive the fixed update rate criterion of Blackman and Van Keuk. The derivation of the criterion is fully explained in section 2.2.

2.1 The Singer model and the linear Kalman Filter

2.1.1 The Singer model

The target dynamics are supposed to be three-dimensional and in Cartesian coordinates. The well-known Singer model, see for example [6] or [25], is a linear model based on the assumption that the acceleration coordinates a_1, a_2, a_3 are all mutually independent Ornstein-Uhlenbeck processes. We have

$$\dot{a}_i(t) = -\alpha a_i(t) + w(t), \quad i = 1,2,3$$

with $w(t)$ a continuous white Gaussian noise, and the autocorrelation of each acceleration coordinate thus writes:

$$E[a_i(t)a_j(t+\tau)] = \delta_{ij}\Sigma^2 e^{-\alpha\tau}$$

with Σ the acceleration noise standard deviation and $1/\alpha$ is the correlation time. Such model accounts for the fact that accelerations in one direction tend to typically last for some time $1/\alpha$, but on average the acceleration of the target is 0. This gives the following discrete evolution equation (1) for each position coordinate i, and between two time instants k and $k+T$. $x = \begin{pmatrix} x_1^T & x_2^T & x_3^T \end{pmatrix}^T$ will be the 9-dimensional state vector.

$$x_i(k+T) = Fx_i(k) + w_k = \begin{pmatrix} 1 & T & \frac{\alpha T - 1 + e^{-\alpha T}}{\alpha^2} \\ 0 & 1 & \frac{1-e^{-\alpha T}}{\alpha} \\ 0 & 0 & e^{-\alpha T} \end{pmatrix} x_i(k) + w_k \tag{1}$$

The process noise covariance matrix Q (from which the Gaussian white noise w_k is drawn) writes $Q = E[w_k w_k^T]$. The expectation can be explicitly computed as a time integral, as shown in the Appendix I of [6], and finally the matrix writes

$$Q = 2\alpha\Sigma^2 \begin{pmatrix} \frac{T^5}{20} & \frac{T^4}{8} & \frac{T^3}{6} \\ \frac{T^4}{8} & \frac{T^3}{3} & \frac{T^2}{2} \\ \frac{T^3}{6} & \frac{T^2}{2} & T \end{pmatrix}$$

Letting $v(k)$ be a Gaussian white noise, radar measurements write:

$$y(k) = Hx(k) + v(k),\ E[v(k)v(k)^T] = N \tag{2}$$

$y(k)$ is the cartesian position measured at time k, and H is the measurement matrix, which writes:

$$H = \begin{pmatrix} H_1 & 0_{1,3} & 0_{1,3} \\ 0_{1,3} & H_1 & 0_{1,3} \\ 0_{1,3} & 0_{1,3} & H_1 \end{pmatrix}$$

with $H_1 = \begin{pmatrix} 1 & 0 & 0 \end{pmatrix}$.

2.1.2 Linear Kalman Filter

With model (1) and measurements (2), one can perform linear Kalman filtering. The equations of the linear Kalman filter are recalled below, where Q and N are the covariance matrices for the process and the measurement noises respectively.

1. Prediction step:

$$\hat{x}(k+1) = F\hat{x}(k)$$
$$P(k+1) = FP(k)F^T + Q(k)$$

2. Update step:

$$z(k) = y(k) - H\hat{x}(k)$$
$$K(k) = P(k)H(HP(k)H^T + N)^{-1}$$
$$\hat{x}^+(k) = \hat{x}(k) + K(k)z(k)$$
$$P^+(k) = (I_9 - K(k)H)P(k)$$

As the considered problem is linear, Gaussian, and time-invariant, the Kalman covariance matrix converges to a fixed value, called P_∞ (see [26]). It turns out that the latter convergence property allows deriving a fixed criterion for the optimization of the update rate.

2.2 Fixed optimal update frequency derivation

In [1], Blackman and Van Keuk propose the following approach to optimize the update frequency in order to minimize radar load. The radar load L_c is defined as

$$L_c = \frac{E(n)}{E(T)}, \tag{3}$$

where $E(n)$ is the average number of illuminations to find a target and T is the duration between two measurements. The problem is feasible, as the more time T we wait between two measurements, the less energy is spent, but the more difficult it is to find the target again, and the average number of illuminations has to be increased to recover sight of the target. It is possible to express $E(n)$ and $E(T)$ as a function of a common variable, V_0 as follows.

To compute (3), one needs to express the covariances in (r,u,v) coordinates where r is the distance of the radar to the target, and u,v are the angles defined as follows:

$$u = \cos el \sin az$$
$$v = \sin el$$

where el and az are the elevation and azimuth angles respectively.

- Estimation of $E(n)$: [1] proposes a way to estimate $E(n)$. As it is not the main concern of this paper, and may depend on the radar and the repointing strategy we will not enter the details of the estimation nor will we discuss the choice of the method to perform the estimations. We will directly use instead the search strategy proposed in [1], as explained in section 3. The strategy is to search the target at the maximum of the pdf of its predicted position in (u,v). If the target is not found at the first illumination, then we compute a slightly modified pdf and try again, until the target is found, or we reach a maximum number of illuminations. This strategy will be detailed more precisely in section 3 where we will use it to develop our adaptive algorithm. The expectation of the number of illuminations to find a target is given by (4), with $\tilde{\alpha} \approx 1 + 14(|\ln P_F|/SN_0)^{1/2}$, and $P_D = P_F^{1/(1+SN_0)}$ where P_F is the probability of false alarm and SN_0 the Signal to Noise Ratio at the center of the beam.

$$E(n) = \frac{1}{P_D}(1 + \tilde{\alpha} V_0^2)^{1/2} \tag{4}$$

- Estimation of $E(T)$: it depends on the chosen target model. For the Singer linear model with Cartesian observations, the covariance matrix converges towards a fixed matrix P_∞ so the variance of the predicted dispersion of the target's position also converges towards a value $\tilde{P}_\infty$, which depends on T, the duration between two measurements (the larger T the larger the eigenvalues of $\tilde{P}_\infty$). It means that at the measurement time, the position of the target can be modelled by a Gaussian random variable of variance $\tilde{P}_\infty$. The formula giving $\tilde{P}_\infty(T)$ can be inverted to get $T(\tilde{P}_\infty)$, which is also a nontrivial property due to the use of the Singer model. The inversion of the formula $\tilde{P}_\infty(T)$ will not be possible with other models indeed.

Using the two latter components, we can evaluate L_c of equation (3) as a function of $\tilde{P}_\infty$. As will be shown in the sequel, this is equivalent to express L_c as a function of V_0.

Van Keuk and Blackman have introduced the quantity V_0 to evaluate the angular precision of the relative prediction with respect to the beamwidth B such that $G(k) = V_0 B$, where $G(k)$ is the principal axis of the 1σ ellipse defined by the covariance matrix of the prediction error at time t_k given by the Kalman filter, and associated to coordinates in the angular (u,v) space. One can assume that the probability distributions of the measurement and the process noise are isotropic in the angular coordinate system (u,v), so the ellipse is in fact a circle. It is then possible to choose arbitrarily any coordinate axis as the principal axis, say, u. $G(k)$ can thus be expressed from the filter's covariance $P(k)$ as follows. Recall that, $\tilde{P}(k) = HP(k)H^T$ is the position covariance matrix according to the filter. We have $G(k) = \sqrt{\tilde{H}_{uv}(k)\tilde{P}(k)\tilde{H}_{uv}(k)^T}$, with $\tilde{H}_{uv}$ the Jacobian of the matrix that relates the Cartesian to spherical (r,u,v) coordinates, i.e.,

$$\tilde{H}_{uv}(k) = \begin{pmatrix} x_1/r & x_2/r & x_3/r \\ \frac{x_2^2+x_3^2}{r^3} & -\frac{x_1 x_2}{r^3} & -\frac{x_1 x_3}{r^3} \\ -\frac{x_1 x_3}{r^3} & -\frac{x_2 x_3}{r^3} & \frac{x_1^2+x_2^2}{r^3} \end{pmatrix} \tag{5}$$

The time between two revisits, which depends on the average number of illuminations necessary to find the targets, also converges to a stable value when the error's variance filter becomes stationary. So let us focus only on the stationary asymptotic phase. Define

$$P_\infty = \lim_{k\to\infty, \alpha T\to 0} P(k).$$

Using the asymptotic Riccati algebraic equation, the stationary position covariance $\tilde{P}_\infty$ is given by (6), where $(.)_{pos}$ extracts the coefficients corresponding to the position variable in the covariance matrix, i.e., $(C)_{pos} := HCH^T$, and $\mathrm{diag}(a)$ is the matrix with a on its diagonal.

$$\tilde{P}_\infty = \left(F(P - PH^T(HPH^T+N)^{-1}HP)F^T\right)_{pos} + \mathrm{diag}(2\alpha\Sigma^2\frac{T^5}{20}) \tag{6}$$

$N = \sigma^2 I_3$ is the measurement covariance matrix. Moreover, as we are only interested in the angular variability, we select the second diagonal element of $\tilde{H}_{uv}(k)\tilde{P}(k)\tilde{H}_{uv}(k)^T$ which is the variance of the asymptotic error in the u variable, hence:

$$G = \sqrt{\left[\tilde{H}_{uv}\tilde{P}_\infty\tilde{H}_{uv}^T\right]_{2,2}} = V_0 B \tag{7}$$

The idea is that $\tilde{P}_\infty$ is a good approximation for the position uncertainty of the radar. The uncertainty in (r,u,v) coordinates is $\tilde{H}_{uv}\tilde{P}_\infty\tilde{H}_{uv}^T$. Since we are only interested in the angular uncertainty, we suppose that r is nearly constant (the same assumption is made in [1] where all formulas depend in fact of r).

Let also $\tilde{C} = \left(F(P - PH^T(HPH^T+N)^{-1}HP)F^T\right)_{pos}$. One can isolate T from equation (6), which gives (8)

$$T = (10)^{1/5}\left(\frac{\sqrt{1/\alpha}}{\Sigma}\right)^{2/5}\left(\tilde{P}_\infty - \tilde{C}\right)^{1/5} \tag{8}$$

Moreover, from (7), and given that the range r is supposed to be approximately constant, we have

$$\tilde{P}_\infty \approx r^2 V_0^2 B^2$$

Finally, (8) becomes

$$T = (10)^{1/5} \left(\frac{\sigma\sqrt{1/\alpha}}{\Sigma/r} \right)^{2/5} \left(\frac{V_0^2 B^2}{\sigma^2} - \frac{\tilde{C}}{\sigma^2 r^2} \right)^{1/5} \tag{9}$$

From now on, let $\nu_0 = \frac{V_0 B}{\sigma}$. Blackman and Van Keuk argue that over a large set of parameters the following approximation is valid

$$T \approx 0.4 P_D \left(\frac{\sigma\sqrt{1/\alpha}}{\Sigma/r} \right)^{0.4} \frac{\nu_0^2}{1+\frac{\nu_0^2}{2}} \tag{10}$$

where P_D is the detection probability, r is the distance between the target and the radar (in m), ξ is the slope factor associated with the mono-pulse measurement process ($\xi = 1.37$). Moreover the measurement noise standard deviation in angular coordinates σ can be expressed as follows:

$$\sigma = \frac{B}{\xi\sqrt{2(SNR+1)}}, \quad SNR \approx \frac{SN_0 - \ln P_F}{1+2V_0^2}$$

Finally, the expression of the radar load L_c is given by (11), with B the half-beamwidth.

$$L_c \approx \left(\frac{\Sigma}{Br\sqrt{1/\alpha}} \right)^{0.4} \frac{1}{P_D} f(V_0, SN_0, P_F) \tag{11}$$

The paper [1] states that for a quite large set of parameters ($SN_0 \in [10, 160]$, $P_F \in [10^{-8}, 10^{-4}]$) the optimal V_0 is 0.3, which gives the optimal revisit period $T = 4.6s$ for $r = 60km, \Sigma = 10m/s^2, \alpha = 1/60s, P_F = 10^{-5}, SN_0 \approx 30(15dB), B = 1^\circ$.

The Blackman Van-Keuk criterion thus gives the optimal track sharpness in the (u, v) space. Whatever the value of the beamwidth, the optimal track sharpness is one sixth of the beamwidth. The revisit time can then be computed on-line thanks to this criterion and to the predicted covariance matrix given by the filtering algorithm, using a smaller time step during the prediction phase.

This is the optimized revisit period for a Singer linear model, and the one sixth of the beamwidth sharpness provides the practitioner with a useful rule of thumb for design purposes, but it should be refined when one wants to use alternative models and filters. In a nonlinear context, the simplifications of the convergent covariance matrix and the inversion of the formula giving $\tilde{P}_\infty$ will no longer be doable, and we have to use numerical integration to derive the optimal revisit time at each time step. The advantage of this method will be to have a totally adaptive revisit time period, that will vary at each time step, and evolve with the measurements, instead of using a fixed criterion. Moreover it is much more versatile, as it suits any model and filtering algorithm, contrary to the previous criterion.

3 Update rate adaptation with a nonlinear model

The Singer model is a specific target model, that dates back to the seventies, and is not pervasively used nowadays. The aim of this section is to propose a generalization of the previous method to any target model, given that the estimation method can provide a predicted covariance matrix whenever it is required. The method of Blackman and Van Keuk to establish a fixed criterion is indeed too simplistic to be applied straightforwardly to any model. However, their initial idea to compute the optimal load with the covariance matrix of the filter can be used to derive another algorithm that can be applied to virtually any filtering algorithm. The computational power to compute a criterion online and to perform the necessary numerical integrations might have been too demanding in the nineties, but can be considered as unproblematic with modern computers.

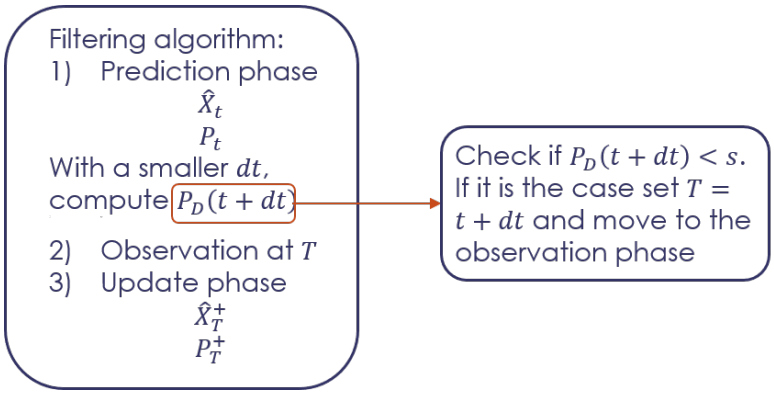

Figure 1: Method used for the adaptive update rate adaptation algorithm

3.1 Method: an adaptive criterion for update rate adaptation

Let us call $P_D(t)$ the detection probability to find a target at a time t. Let us assume that there is a minimum and maximum update rate. The rationale is as follows. We compute the predicted covariance associated to the minimum inter-measurement time, and then increase it gradually until the detection probability drops below a threshold given by client specifications or set by an engineer for example. The method is illustrated by fig. 1. More precisely, we can compute $P_D(t)$ at each time step, and even more often than it is needed. Let us take a smaller time step than the minimum sampling rate. One can integrate the Riccati equation at this short time step and compute the corresponding probability detection easily. A threshold can be used for the probability detection to request a new measurement when it is not satisfying. The new algorithm computes the maximum duration between two measurements, under the constraint that the detection probability, whose computation depends on the number of illuminations, stays high enough. In that sense, it mimics the criterion of Blackman and Van Keuk that minimizes the radar load L_c.

Let us call dT the maximal revisit period between two measurements. We perform covariance prediction every $t+k.dt$, with $k \in \mathbb{N}$ and $dt < dT$. The algorithm to compute the time of the next target revisit is explained in Algorithm 1, where s is the acceptable probability detection threshold. Suppose we are at time t and we want to refresh the measurement to ensure a detection probability $P_D > s$. The next revisit time is called T.

We use the same optimization criterion as in [1], so we allow several illuminations to find a target. We use the same search strategy as for the fixed criterion derivation. This includes expressing the covariance in (u,v) coordinates, the transformation matrix given by (5) in section 2.2, with $r = \sqrt{x_1^2 + x_2^2 + x_3^2}$.

Algorithm 1 Computation of the next revisit time T

Input: $\hat{X}_t, P_t$

while $P_D > s$ and $k < k_{max}$ **do**
  $k := k+1$
  Compute $\hat{X}_{t+k.dt}$ and $P_{t+k.dt}$ with the propagation equations of the filter applied to $\hat{X}_t, P_t$
  Compute H_{uv}, the measurement matrix in the (u,v) space, see (5)
  Compute $\sigma_2 = H_{uv} P_{t+k.dt}(\text{pos}) H_{uv}^T$
  for $n_i = 1$ to N_{max} **do**
    Compute the SNR and the detection probability, according to the number of the illumination n_i: Compute $pdf(n_i)$, find its covariance σ_2 and compute SNR and P_D with (14) and (13)
  end for
  Compute the overall probability detection: $P_D = max(P_D(n_i))$
  Compute the next time revisit: $T = t + k.dt$
end while

Output: T

We also assume that we have an upper bound to the number of illuminations necessary to find a target if the first ones give no detection. This superior bound is called N_{max}. The detection probability also depends on the target search strategy.

3.2 Underlying search strategy

As briefly explained in section 2.2, the search strategy is based on the pdf of the predicted position in (u,v) coordinates. We call this pdf $pdf(1)$. The radar beam points towards the maximum of this pdf in order to maximise the chance to detect the target. If we denote by (u,v) the angles of the beam of the radar and by $(\hat{u},\hat{v})$ the predicted position of the target, then following [1], the Signal-to-Noise Ratio (SNR) can be computed as in (12) to get the detection probability in (13), with P_F the false alarm probability.

$$SNR(u,v) = SN_0 \exp\left(-2\frac{(u-\hat{u})^2 + (v-\hat{v})^2}{B^2}\right) \tag{12}$$

Algorithm 2 Algorithm to perform update rate adaptation for a generic model

1: **while** $T(h) \leq N$ **do**
2: $h := h+1$
3: Apply algorithm 1, which gives $T(h)$, with inputs $\hat{X}^+_{T(h-1)}, P^+_{T(h-1)}$
4: Propagation phase : Compute $\hat{X}_{T(h)}$ and $P_{T(h)}$
5: Request a measurement at time $T(h)$
6: Compute the update $\hat{X}^+_{T(h)}$ and $P^+_{T(h)}$
7: **end while**

$$P_D(u,v) = P_F^{\frac{1}{1+SNR(u,v)}} \tag{13}$$

If the target is not detected on the first illumination, then the pdf is slightly changed into

$$pdf(2)(u,v) := C(1-P_D(u,v))pdf(1)(u,v)$$

The constant is used to normalize the pdf, and of course P_D depends on the position because the SNR does.

We can compute the normalizing constant C of the pdf online, and find its mean μ_2 and covariance σ_2 and thus find the *SNR* with (14) or (12), that permits to compute P_D, with (13) again. This operation can be performed as long as the target is not found, and the maximum number of illuminations N_{max} is not reached either.

$$SNR \approx \frac{SN_0 - \ln(P_F)}{1+2(\sigma_2/B)^2} \tag{14}$$

Let N be the duration of the whole trajectory, T be the function relating the number of the update with the time of the update. The adaptation algorithm is summed up in Algorithm 2.

The main difference between this adaptive method and the regular Blackman and Van Keuk criterion is that in our method, the optimization is performed at each time step, and the update rate is thus perfectly suited to the instantaneous performances of the underlying estimation algorithm. It is possible to link experimentally the detection probability threshold required for the adaptive criterion and the threshold on the covariance matrix in the fixed criterion derivation. This will be explained in greater detail in section 5.

As an application of the proposed method, we use a nonlinear target model, based on the use of the Frenet-Serret frame.

4 Application: Nonlinear target model

In this section we derive a nonlinear model expressed in intrinsic coordinates representing piecewise constant controls in the target frame. It is thus realistic for a large range of flying controlled object. This model is expressed in a Lie group setting, and an appropriate filtering algorithm to perform state estimation is the Invariant Extended Kalman Filter (IEKF) as explained below.

4.1 3D target model in intrinsic coordinates

We still consider the target is evolving in a 3D space. Its motion is described by piecewise constant control commands in a frame that is attached to the aircraft. The idea of expressing the state of the target in a frame attached to it is now a common idea, see [27], [20, 7], see also [28] for robotics applications. For the radar application, and to take into account 3D motions, but accounting for the fact that rotations of the target on itself are unobservable, the Frenet-Serret frame seems most appropriate. The target motion model will thus be derived from the Frenet-Serret frame (T,N,B) evolution formulas. They write

$$\frac{dT}{dt} = u\kappa N, \frac{dN}{dt} = u(-\kappa T + \tilde{\tau} B), \frac{dB}{dt} = -u\tilde{\tau} N \tag{15}$$

u is the norm of the velocity of the centre of the frame. Let us call $\gamma = u\kappa$ and $\tau = u\tilde{\tau}$ the curvature and the torsion of the trajectory respectively (this is slightly different from the mathematical definitions of the curvature and the torsion, κ and $\tilde{\tau}$). If we express the rotation matrix going from the Cartesian frame to the Frenet-Serret frame $R = (T,N,B)$, we can derive the evolution equations (16), assuming that the tangential velocity u, the curvature γ and the torsion τ are approximately constant, and introducing $e_1 = \begin{pmatrix} 1 & 0 & 0 \end{pmatrix}^T$, and $\omega_t = \begin{pmatrix} \tau_t & 0 & \gamma_t \end{pmatrix}$.

The state of the target is composed of the Cartesian position of the target $x_t \in \mathbb{R}^3$, the rotation matrix $R \in SO(3)$, the tangential velocity $u \in \mathbb{R}^+$, the curvature $\gamma \in \mathbb{R}^+$ and the torsion $\tau \in \mathbb{R}^+$, so it is of dimension 9. The notation $(a)_\times$ in equation (16) is explained in the appendix, it refers to the skew-symmetric matrix associated to the 3D vector a. $w_t^x, w_t^\omega, w_t^\gamma, w_t^\tau, w_t^u$ are Gaussian white noises, assumed mutually independent. The target model then writes

$$\begin{cases} \dfrac{dx_t}{dt} = R_t u_t e_1 + w_t^x, & \dfrac{dR_t}{dt} = R_t(\omega_t + w_t^\omega)_\times \\ \dfrac{d\gamma_t}{dt} = 0 + w_t^\gamma, & \dfrac{d\tau_t}{dt} = 0 + w_t^\tau, \quad \dfrac{du_t}{dt} = 0 + w_t^u, \end{cases} \tag{16}$$

whose first line is a matrix and noisy version of (15), and where the second line states the Frenet parameters (γ_t, τ_t, u_t) are approximately constant over time. As underlined in the equation, the state is composed of two relatively different parts. On the one hand, R_t, x_t undergo a nonlinear evolution, and on the other hand γ_t, τ_t, u_t have a linear evolution. Moreover, we can cast R_t and x_t into a matrix Lie group setting, defining

$$\chi_t = \begin{pmatrix} R_t & x_t \\ 0_{1,3} & 1 \end{pmatrix}, \ \zeta_t = \begin{pmatrix} \gamma_t \\ \tau_t \\ u_t \end{pmatrix} \tag{17}$$

χ_t belongs to a matrix Lie group that is called $SE(3)$, it is the group of rotations and translations in 3D, and it can describe the motions of a point in the 3D space. The state has thus a matrix part, χ_t and a vectorial part ζ_t. The equations (16) can thus in turn be rewritten as follows;

$$\frac{d\chi_t}{dt} = \chi_t(\nu_t + w_t^\chi), \quad \frac{d\zeta_t}{dt} = 0 + w_t^\zeta \tag{18}$$

with $w_t^\chi = \begin{pmatrix} w_t^\omega & w_t^x \end{pmatrix}_\times$, $w_t^\zeta = \begin{pmatrix} w_t^\gamma & w_t^\tau & w_t^u \end{pmatrix}^T$, and the matrix ν_t:

$$\nu_t = \begin{pmatrix} 0 & -\gamma_t & 0 & u_t \\ \gamma_t & 0 & -\tau_t & 0 \\ 0 & \tau_t & 0 & 0 \\ 0 & 0 & 0 & 0 \end{pmatrix}$$

For more information about the Lie groups $SO(3)$ and $SE(3)$ and in particular for the expression $(.)_\times$, see the appendix.

The matrix part of the model, assuming that ζ_t is a known input follows a left-invariant evolution equation. We can thus apply an Invariant Extended Kalman filter on the matrix part and a linear Kalman filter on the vectorial part. The resulting algorithm is described in the next section.

4.2 The IEKF algorithm

To derive a Kalman-type algorithm, one needs to define the error associated to the estimation. In the vectorial case where X_t is the state, the error is defined by $\eta_t^X = \hat{X}_t - X_t$, where $\hat{X}_t$ is the estimated state at time t. However this error definition has no sense when it comes to matrix states, and especially when the state lies in a Lie group. Indeed, if χ_1 and χ_2 are two matrices belonging to $SE(3)$, there is no reason why $\chi_1 - \chi_2$ should also belong to $SE(3)$. A more proper and meaningful definition of the matrix error is to consider

$$\eta_t^\chi = \chi_t^{-1}\hat{\chi}_t. \tag{19}$$

Now let us suppose that ζ_t of (17) is known. Then the error evolution equation is autonomous, indeed:

$$\frac{d\eta_t^\chi}{dt} = \eta_t^\chi \nu_t - \nu_t \eta_t^\chi - w_t^\chi \eta_t^\chi \tag{20}$$

does not depend on the predicted state $\hat{\chi}$ at all. If, like in our radar application ζ_t of (17) is not known, then this equation undergoes a slight modification, as detailed below:

$$\frac{d\eta_t^\chi}{dt} = -\chi_t^{-1}\frac{d\chi_t}{dt}\chi_t^{-1}\hat{\chi}_t + \chi_t^{-1}\frac{d\hat{\chi}_t}{dt} = -(\nu_t + w_t^\chi)\eta_t^\chi + \eta_t^\chi \hat{\nu}_t$$

So finally, for an unknown ζ_t of (17), (20) writes:

$$\frac{d\eta_t^\chi}{dt} = \eta_t^\chi \hat{\nu}_t - \nu_t \eta_t^\chi - w_t^\chi \eta_t^\chi.$$

The evolution of ζ remains in the classical setting $\eta_t^\zeta = \hat{\zeta}_t - \zeta_t$, and its evolution is:

$$\frac{d\eta_t^\zeta}{dt} = 0 + w_t^\zeta$$

To be able to express the covariance matrix evolution, the evolution of the linearization of this double error has to be derived. To achieve this, see the preliminary conference

paper [9] that presents the explicit computations in 3D. Let us call ξ_t^χ and ξ_t^ζ the linearized errors associated to η_t^χ and η_t^ζ respectively. If we introduce the linearized error $\xi_t = \begin{pmatrix} \xi_t^\chi & \xi_t^\zeta \end{pmatrix}^T$, then we have the following global linearized error evolution:

$$\frac{d\xi_t}{dt} = A_t \xi_t + w_t$$

with the sparse linearized matrix

$$A_t = \begin{pmatrix} 0 & -\hat{\gamma}_t & 0 & 0 & 0 & 0 & 0 & -1 & 0 \\ \hat{\gamma}_t & 0 & -\hat{\tau}_t & 0 & 0 & 0 & 0 & 0 & 0 \\ 0 & \hat{\tau}_t & 0 & 0 & 0 & 0 & -1 & 0 & 0 \\ 0 & 0 & 0 & 0 & -\hat{\gamma}_t & 0 & 0 & 0 & -1 \\ 0 & 0 & -\hat{u}_t & \hat{\gamma}_t & 0 & -\hat{\tau}_t & 0 & 0 & 0 \\ 0 & \hat{u}_t & 0 & 0 & \hat{\tau}_t & 0 & 0 & 0 & 0 \\ 0 & 0 & 0 & 0 & 0 & 0 & 0 & 0 & 0 \\ 0 & 0 & 0 & 0 & 0 & 0 & 0 & 0 & 0 \\ 0 & 0 & 0 & 0 & 0 & 0 & 0 & 0 & 0 \end{pmatrix}$$

At this point, it becomes easy to adapt the standard Kalman filter equations to our model and error definition. The usual vectorial operations have to be adapted to the Lie group/Lie algebra operations. The algorithm and the adapted operations are described below, it mimics the standard linear Kalman filter presented in section 2.1. We assume noisy Cartesian position measurements $y_{t_n} = x_{t_n} + v_n$, with v_n white Gaussian noise with covariance N. Let H be the measurement matrix, it writes $H = \begin{pmatrix} 0_{3,3} & I_3 & 0_{3,3} \end{pmatrix}$.

1. Prediction step: solve

$$\frac{d\hat{\chi}_t}{dt} = \hat{\chi}_t \hat{\nu}_t \quad \text{and} \quad \frac{d\hat{\zeta}_t}{dt} = 0$$
$$\frac{dP_t}{dt} = A_t P_t + P_t A_t^T + Q_t$$

2. Update step:

$$z_n = \hat{R}_{t_n}^T (y_{t_n} - \hat{x}_{t_n})$$
$$K_n = P_{t_n} H (H P_{t_n} H^T + \hat{R}_{t_n} N \hat{R}_{t_n}^T)^{-1}$$
$$\hat{\chi}_{t_n}^+ = \hat{\chi}_{t_n} \exp((K_n z_n)_{0:5}) \quad \text{and} \quad \hat{\zeta}_{t_n}^+ = \hat{\zeta}_{t_n} + (K_n z_n)_{6:8}$$
$$P_{t_n}^+ = (I_9 - K_n H) P_{t_n}$$

The exp refers to the Lie group exponential, see the appendix.

The use of the error η_t^χ ensures that the covariance matrix evolution does not depend on $\hat{x}_t$ nor on $\hat{R}_t$, as it would be the case for an EKF. Indeed, the EKF uses a linearization of order 1 of the nonlinear evolution function around the predicted state. In 3D, it is moreover very difficult to express the evolution as a vectorial equation, since the rotation matrix has to be replaced by the three rotation angles, that have very nonlinear evolution. Thus, the IEKF is better suited to this target model than the EKF, because of the rotation matrix that can be embedded in a Lie group.

4.3 Expected performances

We can compute approximately the detection probability threshold induced by the use of the fixed criterion to compare with the adaptive criterion, thanks to (21). On a trajectory simulated with a Singer model, the results obtained should be very similar. Indeed, the Singer model and the linear Kalman filter match the hypotheses of section 2.2.

$$P_{D_0} = P_F^{\frac{1}{1+SN_0}} \tag{21}$$

When using the Frenet-Serret based model instead, we anticipate an improvement of the optimization rate L_c when we move from the fixed criterion to the adaptive one. The usefulness of the adaptive method will depend on the size of the improvement. An advantage of the adaptive criterion is also to adapt the detection probability threshold to the requirements of the client. This detection probability could also serve as an indication of the performance of the estimation filter.

Finally, for the fixed as for the adaptive criteria, the update rate adaptation algorithm is very dependant on the quality of the filtering algorithm, since it is based on its results. Indeed if the algorithm provides erroneous covariance predictions, then the update rate computations will be also erroneous. And once again, what we expect of this update rate adaptation is an improvement of the radar load L_c and not of the precision of the estimation. So the filtering algorithm has to be reliable to perform these update rate algorithms. This is why we begin by assessing the performances of the linear Kalman filter on a Singer model trajectory, and the IEKF on a Frenet-Serret model trajectory, with a fixed update rate.

We have performed several experiments to show the differences between the filtering algorithms and the update rate adaptation methods, as described in the next section.

5 Experiments

In this Section, the adaptation algorithm is tested for the two different study cases described in the previous sections. The first study case is the linear Singer model tracked with the linear Kalman filter, and the second study case is the nonlinear Frenet-Serret model tracked with the IEKF. We show the results for the fixed criterion and adaptive algorithms for both cases, and compare the results obtained. The trajectories are built differently for the two models, as will be explained in the following sections.

To begin with, we show the tracking performances of the linear Kalman filter with the Singer model and of the IEKF for the Frenet-Serret model without any update rate adaptation. Then, the update rate will be adaptive and the behaviours of the fixed and adaptive methods along with the radar load will be compared.

5.1 Tracking results with a linear Kalman filter and an IEKF

In this part, we only illustrate the relevance of the models and filters involved, without any concern about the update rate adaptation problem yet.

5.1.1 Tracking with the Singer model with jumps

To test the filters, we first build a trajectory using the Singer model (1): we include one maneuver that occurs at time $t = 200s$, in which the two first coordinates of the acceleration undergo a sudden jump from $a_1 = -0.8m.s^{-2}$ and $a_2 = -0.9m.s^{-2}$ to $a_1 = 2.2m.s^{-2}$ and $a_2 = 2m.s^{-2}$. The position is initially $\begin{pmatrix} x_1 & x_2 & x_3 \end{pmatrix} = \begin{pmatrix} 6000 & 6000 & 6000 \end{pmatrix} m$, and the velocity $\begin{pmatrix} v_1 & v_2 & v_3 \end{pmatrix} = \begin{pmatrix} 0.5 & 0.5 & 0.5 \end{pmatrix} m.s^{-1}$. The parameters for the Singer model are $\alpha = 1/60s^{-1}$ and $\Sigma = 1.0$. The acceleration on the third coordinate does not jump and is initially equal to $a_3 = -0.9m.s^{-2}$. The measurement noise is of variance $1000m$. This trajectory is presented in fig. 2.

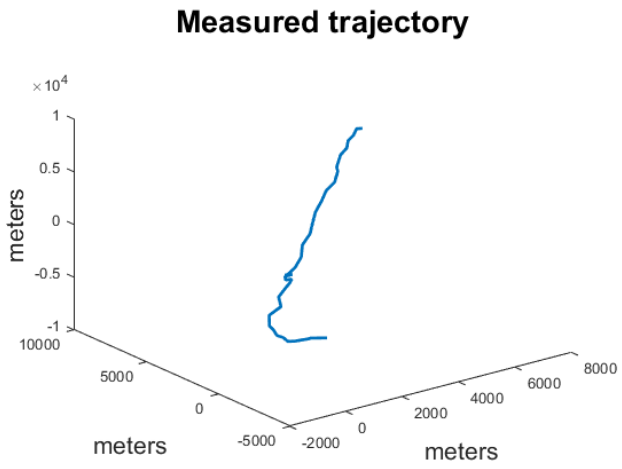

Figure 2: Measured trajectory with the Singer model and one maneuver

The tracking results of the position, the velocity and the acceleration on the first coordinate of the Kalman filter for this trajectory is presented in fig. 3. The update rate is set to be one measurement every ten seconds. The filter estimates quite well the position and the velocity. The estimation of the acceleration is more difficult, especially when the jump occurs. As for all Kalman-based filters, the tuning of the model noise covariance matrix plays a high role in finding a balance between the precision of the estimation and the ability to react efficiently when manoeuvres occur. For further information about noise tuning for Kalman filters, *e.g.* [29], [30].

The lack of precision in the acceleration coordinate is not of crucial importance, as long as it does not result in a reduced precision for the velocity coordinate, which is a parameter that is relevant for some applications (among which intercepting missiles for instance).

5.1.2 Tracking with the Frenet-Serret model with jumps

We test our IEKF algorithm with the trajectory presented in fig. 4. The trajectory is made of three Frenet-parameters constant parts (18). In the first part, the target has

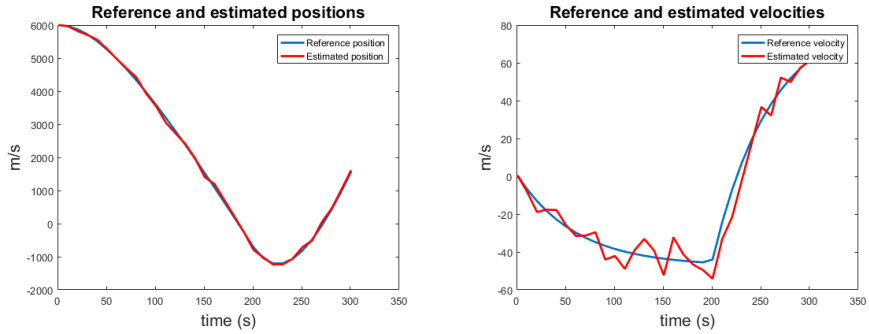

(a) (b)

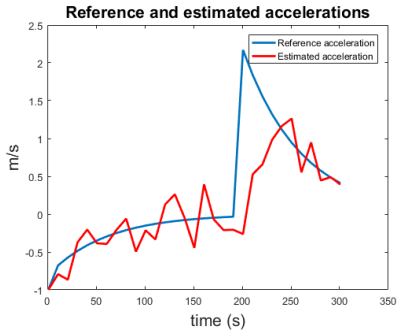

(c)

Figure 3: Results of the linear Kalman filter estimations for the position in x fig. 3a, velocity in x fig. 3b and acceleration in x fig. 3c

a constant velocity straight line motion. In the second part, the target has an helix trajectory, with constant velocity, curvature and torsion, and finally, the target does a constant planar turn. The maneuvers occur at times $t = 200s$ and $t = 450s$ respectively. The initial state is $R_0 = I_3$, $x_0 = \begin{pmatrix} 10^4 & 10^4 & 10^4 \end{pmatrix} m$, $u_0 = 100m.s^{-1}$, $\gamma_0 = 0.02s^{-1}$ and $\tau_0 = 0$. The first jump at $t = 200s$ is characterized by $u_{200} = 500m.s^{-1}$, $\gamma_{200} = 0.07s^{-1}$ and $\tau_{200} = 0.005$, and the second jump by $u_{450} = 200m.s^{-1}$, $\gamma_{450} = 0.002s^{-1}$ and $\tau_{450} = 0$, elsewhere, the velocity, curvature and torsion are constant. We assume Cartesian position measurements, and we add Gaussian measurement noise of variance $1000m$ independently on the three axis.

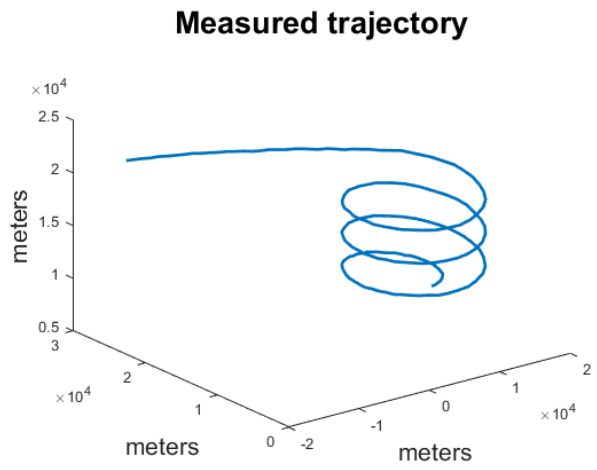

Figure 4: Measured trajectory with two maneuvers

We show the performances of the IEKF, used with a fixed update rate of $T = 5s$. The tracking results of the IEKF alone are presented in fig. 5. We see that the torsion is very difficult to track accurately, indeed, it is a third derivative of the position, and thus it is barely observable. The same problem as the linear Kalman filter with the noise tuning occurs because of the presence of jumps. However once again, the tracking results are satisfying to perform update rate adaptation with the same noise tunings. Indeed, the position and the norm of the velocity, and to a certain extent also the curvature are well estimated with this fixed update rate.

5.2 Update rate adaptation

We now implement the two update rate adaptation methods presented in this paper. The first one uses the fixed Blackman and Van Keuk criterion described in section 2.2, and the second one is the adaptive criterion of algorithm 2. We test the algorithms on the trajectories presented in the previous section, and keep the same process noise tunings for the filtering algorithms.

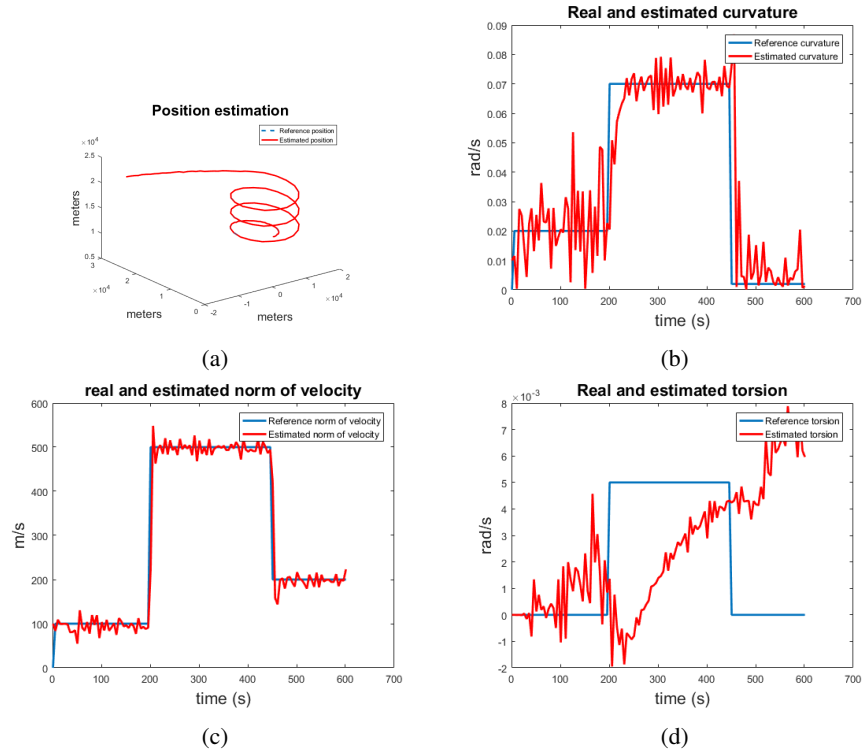

Figure 5: Results for the tracking with the IEKF, with the x position fig. 5a, the curvature fig. 5b, the norm of the velocity fig. 5c and the torsion fig. 5d

5.2.1 Update rate adaptation with the Singer trajectory

We first present the results obtained with the Singer model based trajectory. We compare the fixed criterion with the adaptive one. The Singer model being the model used to compute the fixed criterion, the results should be very similar between both methods. The parameters used for the update rate adaptation for both algorithm are summarized in table 1.

Fixed update criterion The fixed criterion has been first implemented. We plot the duration computed by the algorithm between two measurements as a function of the time elapsed since the beginning of the trajectory. The higher bound for the duration is $T = 10s$ and the lower bound is $T = 0.01s$. The graph for the time interval between measurements is presented in fig. 6a.

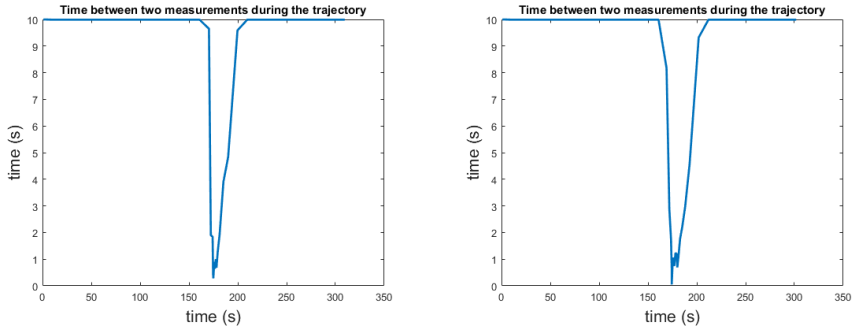

(a) Fixed criterion

(b) Adaptive criterion

Figure 6: Comparison of the duration between two measurements for the Singer model, with the fixed criterion on fig. 6a and for the adaptive criterion fig. 6b. We see the behaviour of the adaptation is very similar for the two criteria. This was expected since the fixed criterion is derived for a Singer model. The peak corresponds to the moment the target becomes very close to the radar, so the angular covariance becomes large.

We can note that the adaptation is not necessarily linked to the presence of a maneuver (the update rate decreases before the maneuver occurs). In fact, it is due to an increase of the covariance in the u-coordinate at $t = 175s$, becomes the target is very close the radar at this point, and we consider the angular dispersion. Let us now compare this behaviour to the one obtained with the adaptive algorithm described in this paper.

Adaptive criterion We make the same experiment, but we replace the fixed criterion with the adaptive one of algorithm 2, and plot the result in fig. 6b. In order to achieve this, we compute the detection probability P_D that corresponds to $V_0 = 0.3$ thanks to the formula $P_{D_0} = P_F^{1/(1+SN_0)}$, which gives the threshold in algorithm 1 to be $s = 0.72$.

We also plot the lateral position covariances for both algorithms in fig. 7. The duration general form curve echoes the covariance curve. When the covariance is low,

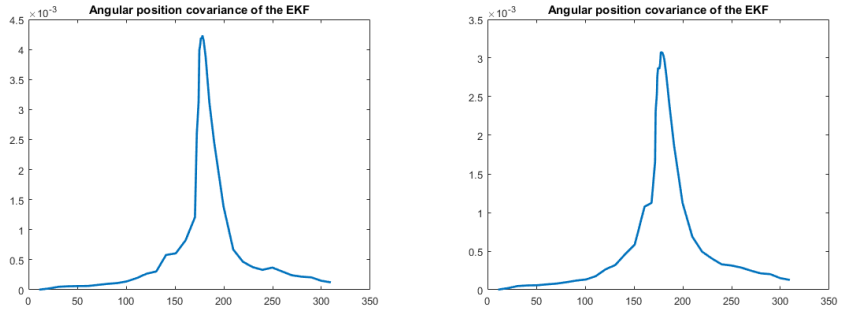

(a) Fixed criterion

(b) Adaptive criterion

Figure 7: Comparison of the covariances for the angular coordinate for the Singer model, with the fixed criterion on fig. 7a and for the adaptive criterion fig. 7b.

then the maximum duration between two measurements is reached (in the first 150 seconds for instance).

As expected, the update rate is very similar in both cases. Indeed, the fixed criterion is adapted to this Singer model, and the adaptive criterion is designed to match any model formulation. This shows our method encompasses and generalizes the model of Blackman and Van Keuk indeed.

Optimization ratio We have performed 100 Monte-Carlo experiments to compute the value of the rate $L_c = E(n)/E(T)$ for both methods in order to compare them. The loads L_c computed are given in table 2. The small difference is due to the approximations that are made in the fixed criterion derivation, and also to the fact that we are not necessarily in a stationary regime during all the trajectory, but the results are nevertheless very similar. We also collect the position estimation Root Mean Square Error, to ensure there is no major degradation of performance when using the adaptive criterion. Indeed, the radar load is optimized, but the tracking performances need to stay at least in the same magnitude order. The RMSE can be found in table 3.

5.2.2 Update rate adaptation with the Frenet-Serret trajectory

The present experiment serves as an example for other models than the Singer model, that are nonlinear, have to be estimated using a nonlinear filtering algorithm and cannot have the same properties of convergence than the linear Kalman filter. The duration between two consecutive measurements can vary from $T_{max} = 5s$ to $T_{min} = 0.005s$. We perform again the simulations with the Blackman Van Keuk fixed criterion and with the adaptive algorithm. The results are presented in the following paragraphs. The values of the other parameters are gathered in table 1.

Fixed criterion The results are given on fig. 8a and fig. 9a. We can allow the duration between the measurements up to $T = 5s$ on some portions of the trajectory.

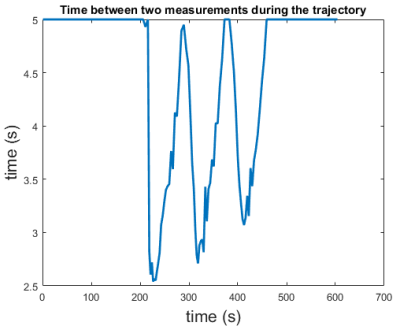

(a) Fixed criterion

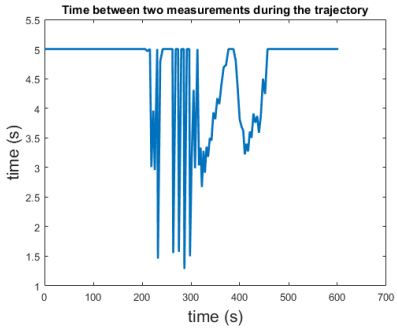

(b) Adaptive criterion

Figure 8: Comparison of the duration between two measurements for the Frenet-Serret model, with the fixed criterion on fig. 8a and the adaptive one on fig. 8b. The experiments give two different behaviours of the duration between two observations. Indeed, the fixed criterion is not suited to this model, and the adaptive criterion is required, as it directly minimizes L_c, contrary to the fixed criterion

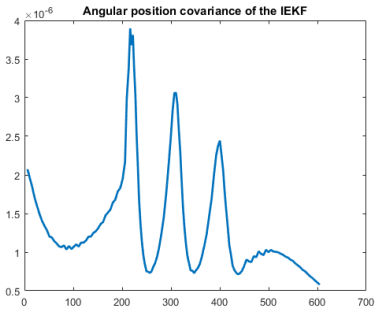

(a) Fixed criterion

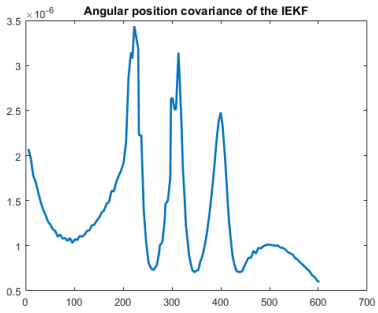

(b) Adaptive criterion

Figure 9: Comparison of the covariances for the angular coordinate for the Frenet-Serret model, with the fixed criterion on fig. 9a and for the adaptive criterion fig. 9b.

Parameter	Value
P_F	10^{-6}
SN_0	40
B	0.0175
s	0.72

Table 1: Parameters for the update rate adaptation

Adaptive criterion Thanks to (21), we can compute the threshold $s = 0.72$ that we apply for the adaptive algorithm. The results are presented in fig. 8b. The angular covariances are also displayed in fig. 9. In this case, the covariances computed are still very similar, because they are the result of the filter, and the difference is due to the period of refreshment.

However, contrary to the Singer model, the update rate results are quite different. The duration between maneuvers is often lower for the adaptive criterion, however, the number of necessary illuminations to find a target again is also lower. We see that the two algorithms lead to two different strategies, even though the general form of the adaptation is the same.

Optimization ratio The optimization rate L_c is again computed with 100 Monte-Carlo simulations for the fixed and adaptive algorithms. The radar loads L_c obtained for the Frenet-Serret model are again collected in table 2. This shows that the optimization is much better with an adaptive criterion, and that the fixed criterion is not sufficient to perform a proper update rate adaptation algorithm. The difference between the rates multiplied by the number of possible targets in a challenging scenario is therefore not negligible at all. The position RMSE are also collected in table 3, again no loss in the performances is observed.

	Fixed criterion	Adaptive criterion
Linear model (Kalman filter)	0.20	0.16
Nonlinear model (IEKF)	0.44	0.25

Table 2: Radar load L_c computed for the experiments presented in this paper

	Fixed criterion	Adaptive criterion
Linear model (Kalman filter)	120	70
Nonlinear model (IEKF)	105	104

Table 3: Position RMSE (in m) computed for the experiments presented in this paper

6 Discussion

The results obtained in the previous section show that the fixed criterion of Blackman and Van Keuk and the adaptive criterion proposed in this paper are equivalent for the Singer model. However, with nonlinear target models, the adaptive algorithm performs better than the fixed one as anticipated. This saves the radar beam time budget: the update rate can be more decreased than when it is fixed, and the adaptive criterion algorithm is better suited to nonlinear models and algorithms than the fixed one.

However, such adaptation algorithms can only adapt the update rate once the performances are beginning to decrease, it is thus not suited to detect or track high and abrupt maneuvers. It is designed to detect a degradation in the filter's confidence of its own estimations, and to increase the update rate, so that the filter is updated more often, and the target has a higher probability to be in the radar beam for the next measurement, and so less energy is spent to find it again. Moreover, the covariance of the filter needs to be quite accurate, since it feeds the update rate adaptation algorithm. If the filter diverges, this means the covariance is not accurate anymore, so the update rate adaptation fails along with the filter.

This is corroborated by the results obtained in the previous section. Indeed, the update rate is not necessarily modified only during maneuvers, but more generally whenever the covariance of the filtering algorithm is increasing.

7 Conclusion

In this paper, we have first recalled the equations of the Singer model and of the linear Kalman filter. We have pedagogically explained the derivation of the criterion of [1]. This criterion being fit only to the particular Singer model, we have adapted it to suit other types of models and estimation algorithms. This is required for industrial applications, since nonlinear target models are used. We have then applied the algorithm proposed to a model based on intrinsic coordinates, relying on the Frenet-Serret frame, along with an Invariant Extended Kalman Filter, which possess more stability properties than the standard EKF. The results both with the Singer model and the Frenet-Serret model corroborate the accuracy of the adaptive algorithm. The fixed and adaptive algorithms give the same results on the Singer model, and the adaptive algorithm gives better results on the Frenet-Serret model.

To develop the adaptive update rate algorithm, we have used the same optimization criterion as in [1]. This criterion assumes the radar has a pencil beam, and the target search method is to look in a neighbourhood of the first guess given by the estimation algorithm. This search method is the optimal one, as stated in [1], so the same search method is used in this paper. These two assumptions have not be questioned in the paper, but future work would be to have another optimization function to take into account the new possibilities of the newer generations of radars ,that are becoming even more cognitive, including the fact that future radars will not necessarily be equipped with pencil beams, and so the radar load will have to be expressed differently.

Acknowledgments

This work is supported by a DGA-MRIS scholarship. The authors would also like to thank G. Foliard and F. Gosselin for their precious help, and the DGA tracker expert F. Livernet.

References

[1] G. van Keuk and S. S. Blackman, "On phased-array radar tracking and parameter control," *IEEE Transactions on Aerospace Electronic Systems*, vol. 29, pp. 186–194, 1993.

[2] S. Haykin, "Cognitive radar: a way of the future," *IEEE Signal Processing Magazine*, vol. 23, no. 1, pp. 30–40, Jan 2006.

[3] M. S. Greco, F. Gini, P. Stinco, and K. Bell, "Cognitive radars: A reality?" *arXiv preprint arXiv:1803.01000*, 2018.

[4] Y. Briheche, F. Barbaresco, F. Bennis, and D. Chablat, "Update rates constraints in fixed-panel radar search pattern optimization with limited time budget," in *Radar Symposium (IRS), 2017 18th International*. IEEE, 2017, pp. 1–10.

[5] Y. Briheche, F. Barbaresco, F. Bennis, D. Chablat, and F. Gosselin, "Non-uniform constrained optimization of radar search patterns in direction cosines space using integer programming," in *Radar Symposium (IRS), 2016 17th International*. IEEE, 2016, pp. 1–6.

[6] R. A. Singer, "Estimating optimal tracking filter performance for manned maneuvering targets," *IEEE Transactions on Aerospace and Electronic Systems*, no. 4, pp. 473–483, 1970.

[7] S. J. Godsill, J. Vermaak, W. Ng, and J. F. Li, "Models and algorithms for tracking of maneuvering objects using variable rate particle filters," *Proceedings of the IEEE*, vol. 95, no. 5, pp. 925–952, 2007.

[8] A. Barrau and S. Bonnabel, "The invariant extended kalman filter as a stable observer," *IEEE Transactions on Automatic Control*, vol. 62, no. 4, pp. 1797–1812, 2017.

[9] M. Pilté, S. Bonnabel, and F. Barbaresco, "Tracking the frenet-serret frame associated to a highly maneuvering target in 3d," in *2017 IEEE 56th Annual Conference on Decision and Control (CDC)*, Dec 2017, pp. 1969–1974.

[10] Y. Bar-Shalom, X. Li, and T. Kirubarajan, *Estimation with Applications to Tracking and Navigation: Theory Algorithms and Software*. Wiley, 2004. [Online]. Available: https://books.google.fr/books?id=xz9nQ4wdXG4C

[11] S. J. Julier and J. K. Uhlmann, "New extension of the kalman filter to nonlinear systems," in *AeroSense'97*. International Society for Optics and Photonics, 1997, pp. 182–193.

[12] ——, "Unscented filtering and nonlinear estimation," *Proceedings of the IEEE*, vol. 92, no. 3, pp. 401–422, 2004.

[13] A. Doucet, S. Godsill, and C. Andrieu, "On sequential Monte Carlo sampling methods for bayesian filtering," *Statistics and Computing*, vol. 10, no. 3, pp. 197–208.

[14] A. Doucet, N. De Freitas, K. Murphy, and S. Russell, "Rao-blackwellised particle filtering for dynamic bayesian networks," in *Proceedings of the Sixteenth conference on Uncertainty in artificial intelligence*. Morgan Kaufmann Publishers Inc., 2000, pp. 176–183.

[15] S. A. Cohen, "Adaptive variable update rate algorithm for tracking targets with a phased array radar," *Communications, Radar and Signal Processing, IEE Proceedings F*, vol. 133, no. 3, pp. 277–280, June 1986.

[16] G. A. Watson and W. D. Blair, "Tracking performance of a phased array radar with revisit time controlled using the imm algorithm," in *Proceedings of 1994 IEEE National Radar Conference*, Mar 1994, pp. 160–165.

[17] H. Benoudnine, M. Keche, A. Ouamri, and M. Woolfson, "Fast adaptive update rate for tracking a maneuvering target with a phased array radar, using imm and mrimm algorithms," *Journal of Applied Science*, vol. 9, no. 2, 2009.

[18] P. Sarunic, "Adaptive update rate target tracking for a phased array radar," Master's thesis, University of South Australia, 1995.

[19] H. J. Shin, S. M. Hong, and D. H. Hong, "Adaptive-update-rate target tracking for phased-array radar," *IEE Proceedings - Radar, Sonar and Navigation*, vol. 142, no. 3, pp. 137–143, Jun 1995.

[20] S. Godsill and J. Vermaak, "Variable rate particle filters for tracking applications," in *IEEE/SP 13th Workshop on Statistical Signal Processing, 2005*. IEEE, 2005, pp. 1280–1285.

[21] M. Basseville, I. V. Nikiforov *et al.*, *Detection of abrupt changes: theory and application*. Prentice Hall Englewood Cliffs, 1993, vol. 104.

[22] J. Korn, S. W. Gully, and A. S. Willsky, "Application of the generalized likelihood ratio algorithm to maneuver detection and estimation," in *1982 American Control Conference*, June 1982, pp. 792–798.

[23] C. Alippi and M. Roveri, "An adaptive cusum-based test for signal change detection," in *2006 IEEE International Symposium on Circuits and Systems*, May 2006, pp. 4 pp.–.

[24] M. Pilté and F. Barbaresco, "Tracking quality monitoring based on information geometry and geodesic shooting," in *Radar Symposium (IRS), 2016 17th International*. IEEE, 2016, pp. 1–6.

[25] Y. Bar-Shalom, P. K. Willett, and X. Tian, *Tracking and data fusion*. YBS publishing, 2011.

[26] B. R. S. Kalman, R. E., "New results in linear filtering and prediction theory," *J. Basic Eng.*, 1961.

[27] M. Pilté, S. Bonnabel, and F. Barbaresco, "An innovative nonlinear filter for radar kinematic estimation of maneuvering targets in 2d," in *Radar Symposium (IRS), 2017 18th International*. IEEE, 2017, pp. 1–10.

[28] A. Barrau and S. Bonnabel, "Intrinsic filtering on lie groups with applications to attitude estimation," *IEEE Transactions on Automatic Control*, vol. 60, no. 2, pp. 436–449, 2015.

[29] P. Matisko and V. Havlena, "Noise covariances estimation for kalman filter tuning," *IFAC Proceedings Volumes*, vol. 43, no. 10, pp. 31 – 36, 2010, 10th IFAC Workshop on the Adaptation and Learning in Control and Signal Processing. [Online]. Available: http://www.sciencedirect.com/science/article/pii/S1474667015323351

[30] B. M. Åkesson, J. B. Jørgensen, N. K. Poulsen, and S. B. Jørgensen, "A tool for kalman filter tuning," in *17th European Symposium on Computer Aided Process Engineering*, ser. Computer Aided Chemical Engineering, V. Pleşu and P. Şerban Agachi, Eds. Elsevier, 2007, vol. 24, pp. 859 – 864.

Appendix: Matrix Lie Groups

General definitions

A matrix Lie group G is a set of invertible matrices, stable by multiplication and inversion, and differentiable. The differentiability allows to define the Lie algebra $\mathfrak{g}$ associated to the group, which is the tangent space at the neutral element. The Lie algebra is an $\mathbb{R}$-algebra, which means that it is a vectorial space with an intern multiplication which is bilinear. For a matrix Lie group, it is possible to represent the vectors of the Lie algebra under the form of a matrix, that is strictly equivalent, but may be more convenient to write the operations.

Group of 3D rotations $SO(3)$

The group of rotations $SO(3)$ is composed of the rotation matrices of dimension 3×3: $SO(3) = \{R \in \mathscr{M}_3 | RR^T = R^T R = I_3, \det(R) = 1\}$. The associated Lie algebra is of

dimension 3 and is defined by:

$$\mathfrak{so}(3) = \left\{ \begin{pmatrix} 0 & -c & b \\ c & 0 & -a \\ -b & a & 0 \end{pmatrix}, \begin{pmatrix} a \\ b \\ c \end{pmatrix} \in \mathbb{R}^3 \right\}$$

It is now possible to define the notation $(.)_\times$. This notation comes from the fact that there exists a bijection between $\mathfrak{so}(3)$ and $\mathbb{R}^3$. And an element of $\mathfrak{so}(3)$ can be equivalently represented by a vector in $\mathbb{R}^3$. The bijection is denoted $(.)_\times$. If $\omega \in \mathbb{R}^3$, then

$$(\omega)_\times = \begin{pmatrix} 0 & -\omega_3 & \omega_2 \\ \omega_3 & 0 & -\omega_1 \\ -\omega_2 & \omega_1 & 0 \end{pmatrix}$$

One also needs the definition of the matrix exponential $\exp : \mathfrak{so}(3) \to SO(3)$. Let $\Omega \in \mathfrak{so}(3)$, and $\theta = \|\Omega\|$. The exponential map is:

$$\exp(\Omega) = I_3 + \frac{\sin\theta}{\theta}\Omega + \frac{1-\cos\theta}{\theta^2}\Omega^2$$

Group of 3D rotations and translations $SE(3)$

$SE(3)$ is the group that describes the possible motions of point mass in the 3D space. It represents the rotations and the translations:

$$SE(3) = \left\{ \begin{pmatrix} R & x \\ 0_{1,3} & 1 \end{pmatrix}, R \in SO(3), x \in \mathbb{R}^3 \right\}$$

The associated Lie algebra is of dimension 6 and is defined by:

$$\mathfrak{se}(3) = \left\{ \begin{pmatrix} 0 & -c & b & \alpha \\ c & 0 & -a & \beta \\ -b & a & 0 & \gamma \\ 0 & 0 & 0 & 0 \end{pmatrix}, \begin{pmatrix} a \\ b \\ c \end{pmatrix} \in \mathbb{R}^3, \begin{pmatrix} \alpha \\ \beta \\ \gamma \end{pmatrix} \in \mathbb{R}^3 \right\}$$

The exponential map of $(\omega, u) \in \mathbb{R}^3 \times \mathbb{R}^3$ is defined as follows

$$\exp \begin{pmatrix} (\omega)_\times & u \\ 0 & 0 \end{pmatrix} = \begin{pmatrix} \exp((\omega)_\times) & Vu \\ 0 & 1 \end{pmatrix}$$

with $\theta = \sqrt{\omega^T \omega}$ and

$$V = I_3 + \frac{1-\cos\theta}{\theta^2}(\omega)_\times + \frac{\theta - \sin\theta}{\theta^3}(\omega)_\times^2$$